Quantum dynamics of a single fluxon in Josephson-junction parallel arrays with large kinetic inductances

S. S. Seidov [1] and M. V. Fistul [1,2,3]

[1] *National University of Science and Technology "MISIS", Moscow 119049, Russia*
[2] *Russian Quantum Center, Skolkovo, Moscow 143025, Russia*
[3] *Theoretische Physik III, Ruhr-Universität Bochum, Bochum 44801, Germany*

(Received 15 January 2021; accepted 21 May 2021; published 8 June 2021)

We present a theoretical study of coherent quantum dynamics of a single magnetic fluxon (MF) trapped in Josephson-junction parallel arrays (JJPAs) with large kinetic inductances. The MF is the topological excitation carrying one quantum of magnetic flux, Φ_0. The MF is quantitatively described as the 2π kink in the distribution of Josephson phases, and for JJPAs with high kinetic inductances the characteristic length of such distribution (the "size" of MF) is drastically reduced. Characterizing such MFs by the Josephson phases of three consecutive Josephson junctions we analyze the various coherent macroscopic quantum effects in the MF quantum dynamics. In particular, we obtain the MF energy band originating from the coherent quantum tunneling of a single MF between adjacent cells of JJPAs. The dependencies of the band width Δ on the Josephson coupling energy E_J, charging energy E_C and the inductive energy of a cell E_L, are studied in detail. In long linear JJPAs the coherent quantum dynamics of MF demonstrates decaying quantum oscillations with characteristic frequency $f_{qb} = \Delta/h$. In short annular JJPAs the coherent quantum dynamics of MF displays complex oscillations controlled by the Aharonov-Casher phase $\chi \propto V_g$, where V_g is an externally applied gate voltage. In the presence of externally applied dc bias, I, a weakly incoherent dynamics of quantum MF is realized in the form of macroscopic Bloch oscillations leading to a typical "nose" current-voltage characteristics of JJPAs. As ac current with frequency f is applied the current-voltage characteristics display a set of equidistant current steps at $I_n = 2enf$.

DOI: 10.1103/PhysRevA.103.062410

I. INTRODUCTION

Great attention has been devoted to a study of solitons, i.e., stable spatially distributed macroscopic structures formed in different nonlinear media [1]. The solitons have been obtained in various complex solid-state, optical, chemical, and biological systems [2,3]. An interesting example of topological solitons [4] are so-called *magnetic fluxons* (MFs) found in low-dimensional superconducting systems, e.g., two-dimensional Josephson-junction arrays, long Josephson junctions or Josephson-junction parallel arrays [5,6]. Such MFs are vortices of persistent superconducting current, each of them carrying one quantum of magnetic flux, Φ_0.

An ideal experimental platform to study the classical dynamics of MFs is Josephson-junction parallel arrays (JJPAs). A single MF can be trapped in such systems and the dynamics of MF is controlled by externally applied current bias. A large amount of fascinating physical effects in the dynamics of MFs has been theoretically predicted and experimentally observed, e.g., dc current induced resonances [5], the relativistic dynamics of MF [6], bunching of MFs [7], the Cherenkov radiation of plasma modes by moving MF [8], ac current induced dynamic metastable states [9], just to name a few. From mathematical point of view the classical dynamics of MF is determined by a large set of coupled nonlinear differential equations [6] and a single MF is described as 2π kink in the spatial distribution of Josephson phases [5,6].

The next question that naturally arises in this field is: Is it possible to obtain macroscopic coherent quantum-mechanical phenomena in the dynamics of topological magnetic fluxons? Indeed, the incoherent macroscopic quantum tunneling of magnetic vortices has been theoretically analysed [10] and observed in two-dimensional Josephson-junction arrays [11], macroscopic quantum tunneling, and energy level quantization of a single MF have been theoretically studied [12–15], and it has been observed in the dynamics of a single MF trapped in a long Josephson junction [16]. Notice here that in all these works the size of MF greatly exceeded a typical size of artificially prepared potential, e.g., a cell size of JJPAs, and therefore, the continuous limit was used. However, coherent quantum effects in the dynamics of MFs have not been observed yet.

Observation of coherent quantum dynamics of topological MFs is hampered by severe obstacles: unavoidably present dissipation, decoherence, and low-frequency offset charge noise induced by fluctuating charged impurities on small superconducting islands [17,18], and a large size of MF formed in JJPAs with low (geometrical) inductances, not allowing us to map the initial many-body problem to the quantum dynamics of a single degree of freedom. However, an intensive study of various superconducting lumped elements biased in quantum regime, i.e., superconducting qubits, and networks of interacting superconducting qubits, has already resulted in a substantial reduction of dissipation and

decoherence [19]. A second problem of reducing the size of MF can be solved by replacement of low geometrical inductances with large kinetic inductances that allows us to shrink the 2π kink distribution. Moreover, in such JJPAs all small superconducting islands are shunted by large kinetic inductances and, therefore, the offset charge noise is drastically reduced [20]. Large kinetic inductances can be implemented in JJPAs by two methods: embedding in each cell of JJPAs series arrays of large Josephson junctions [20–23], or using disordered superconducting materials [24–26]. Recently, some coherent quantum-mechanical effects in the dynamics of MFs trapped in JJPAs with high kinetic inductances were theoretically studied in Ref. [27].

In this paper we systematically study the *coherent quantum dynamics* of a single MF trapped in JJPAs with large kinetic inductances. The large kinetic inductance is provided by series arrays of large Josephson junctions, and thus, the size of MF becomes much smaller than the cell size. In this case that is close to *anticontinuous* limit [28] we obtain explicitly that the dynamics of MF is determined by the collective coordinate, i.e., a single degree of freedom. By making use of a previously well-elaborated analysis of the coherent quantum dynamics of a single degree of freedom we study in detail the MF energy spectrum originating from the macroscopic quantum tunneling in the effective intrinsic Peierls-Nabarro potential, and the coherent quantum oscillations (quantum beats) of MFs occurring in long linear and short annular JJPAs. We show that the frequency of quantum oscillations obtained in short annular JJPAs can be controlled by the Aharonov-Casher phase [29]. In the presence of externally applied dc bias current and taking into account a weak dissipation we obtain Bloch oscillations [30,31] in the dynamics of a single MF.

The paper is organized as follows. In Sec. II we present our model for JJPAs with large kinetic inductances, derive the total Lagrangian of such a system. In Sec. III we provide a macroscopic quantum-mechanical description of the coherent quantum dynamics of a single fluxon trapped in such JJPAs. For that we elaborate a special approximation where a single fluxon is characterized by Josephson phases of three consecutive Josephson junctions. In Sec. IV we apply this generic description to analyze in detail various macroscopic quantum phenomena occurring in the dynamics of a single magnetic fluxon, i.e., the MF energy bands, decaying macroscopic quantum oscillations in long linear JJPAs, macroscopic quantum beats controlled by the Aharonov-Cashier phase in short annular JJPAs. In Sec. V a weakly incoherent quantum dynamics of MF in the presence of dc and ac bias currents is discussed. The Sec. VI provides conclusions.

II. JJPAS WITH LARGE KINETIC INDUCTANCES: MODELS AND LAGRANGIAN

We consider JJPAs with large kinetic inductance composed of M superconducting cells coupled by small Josephson junctions (it is indicated in Fig. 1 by blue crosses). The classical dynamics of such JJPAs is determined by a set of time-dependent Josephson phases, $\varphi_i(t)$. In the presence of

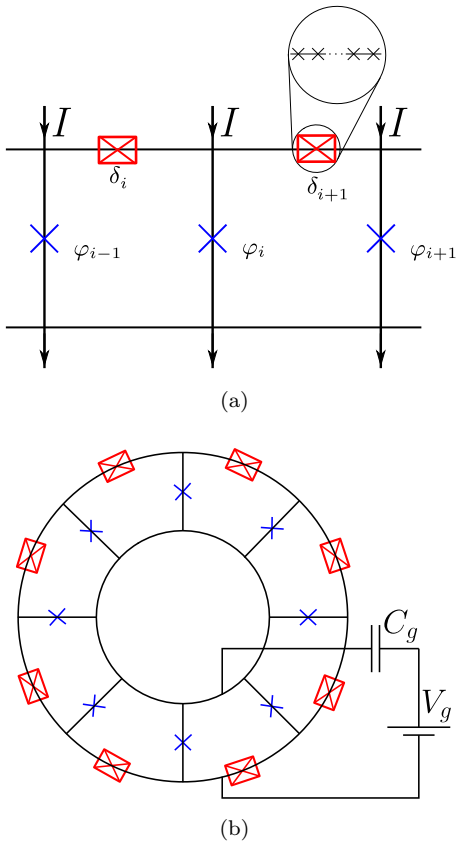

FIG. 1. The schematics of JJPAs with large kinetic inductances: (a) a linear JJPA; (b) an annular JJPA. The bias dc current I and the gate voltage, V_g together with the capacitance C_g are shown. The Josephson phases of small (φ_i), and large (δ_i) Josephson junctions are indicated.

a single MF trapped in a JJPA, the Josephson phases vary from zero to 2π on the whole length of JJPA. In order to observe the quantum-mechanical effects in the MF dynamics, the parameters of small Josephson junctions have to be chosen as $E_J \geqslant E_C$, where E_J and E_C are the Josephson coupling energy and the charging energy, accordingly. A high kinetic inductance of JJPAs is provided by embedding of series arrays of N large Josephson junctions in the upper branch of each cell [20,21] (it is indicated in Fig. 1 by red boxes). The Josephson coupling energy E_{Ja}, and the charging energy E_{Ca} of these large Josephson junctions were chosen as $E_{Ja} \gg E_{Ca}$ in order to suppress the quantum phase slips in series arrays. The dynamics of Josephson junctions built in series arrays is characterized by the time-dependent Josephson phases, δ_i. Each cell is pierced by an externally applied magnetic flux Φ_i, and the dc current I is applied in each node. The schematics of various JJPAs are presented in Fig. 1(a) (the linear JJPA) and Fig. 1(b) (the annular JJPA). Notice here, that in JJPAs of annular form [see Fig. 1(b)], the quantum dynamics of MF can be controlled by an externally applied gate voltage V_g inducing an additional charge on the central superconducting island. Here, C_g is the gate capacitance.

By making use of the Kirhhoff's circuit laws we write the Lagrangian of the system in the following form

[32]:

$$L = K[\dot{\varphi}_i;\dot{\delta}_i] - U[\varphi_i;\delta_i]$$
$$= \sum_{i=1}^{M} \frac{E_J\left(\dot{\varphi}_i - \frac{2eC_g}{\hbar C}V_g\right)^2}{2\omega_p^2} + \frac{E_{Ja}\dot{\delta}_i^2}{2\omega_{pa}^2}$$
$$- E_J(1-\cos\varphi_i) - E_J\frac{I}{I_c}\varphi_i - NE_{Ja}(1-\cos\delta_i), \quad (1)$$

where $\omega_p = \sqrt{8E_JE_C}/\hbar$ and $\omega_{pa} = \sqrt{8E_{Ja}E_{Ca}}/\hbar$ are the plasma frequencies of small and large Josephson junctions, accordingly; I_c is the critical current of a Josephson junction; C is the capacitance of small Josephson junctions. The magnetic flux quantization in each cell leads to a set of constraints on the Josephson phases φ_i and δ_i [33]:

$$N\delta_i + \varphi_{i+1} - \varphi_i = 2\pi\left[n_i + \frac{\Phi_i}{\Phi_0}\right], \quad i = 1,\dots M, \quad (2)$$

where Φ_0 is the magnetic flux quantum, and n_i is a number of magnetic flux quanta penetrating the ith cell. Using such constraints and excluding the phases δ_i from (1) we obtain for the potential energy U the following expression:

$$U(\{\varphi_i\}) = E_J\sum_{i=1}^{M}(1-\cos\varphi_i) + E_J\frac{I}{I_c}\varphi_i$$
$$+ NE_{Ja}\sum_{i=1}^{M}\left(1-\cos\left[\frac{\varphi_i-\varphi_{i+1}}{N} + \frac{2\pi(n_i+\Phi_i)}{\Phi_0 N}\right]\right). \quad (3)$$

As $N \gg 1$ expanding the second term in Eq. (3) up to the second order in $1/N$ we obtain the potential energy

$$U(\{\varphi_i\}) = E_J\sum_{i=1}^{M}(1-\cos\varphi_i) + E_J\frac{I}{I_c}\varphi_i$$
$$+ E_L\sum_{i=1}^{M}\left(\varphi_i - \varphi_{i+1} + 2\pi\frac{(n_i+\Phi_i)}{\Phi_0}\right)^2, \quad (4)$$

where the inductive energy $E_L = E_{Ja}/(2N)$.

III. QUANTUM DYNAMICS OF A SINGLE MF TRAPPED IN A HIGHLY INDUCTIVE ($E_J \gg E_L$) JJPA

Next, we study a particular case, $E_{Ja} \gg E_J$ and $E_C \ll E_{Ca}$, as the quantum dynamics of the Josephson junctions built in series arrays is strongly suppressed. It results in the absence of both the plasma oscillations and macroscopic quantum tunneling (quantum phase slips) in Josephson junctions of series arrays, and therefore, one can neglect the charging energies of series arrays of Josephson junctions in (1), and set all n_i to zero in (4). In arbitrary JJPAs a single trapped MF is described as 2π kink in the distribution of Josephson junctions phases, φ_i, and for low inductive JJPAs ($E_J \ll E_L$) such distribution spreads over many cells. Here, we assume that JJPAs are highly inductive ones, i.e., $E_J \gg E_L$, and the spatial distribution of Josephson phases becomes a sharp one. In this case we use a particular approach elaborated previously to study the classical dynamics of macroscopic topological objects in so-called anticontinuous limit [28,34–36] as a single MF is characterized by the Josephson phases of three consecutive Josephson junctions, and other Josephson phases close to zero or 2π. More precisely, we present the MF as a particular static Josephson phase configuration: $\{\varphi_i\}_{\rm MF} = \{0,\dots,\varphi_{k-1},\varphi_k,2\pi-\varphi_{k+1},\dots,2\pi\}$ where the Josephson phases $\varphi_{k\pm1}$ are small. Such distribution is schematically presented in Fig. 2.

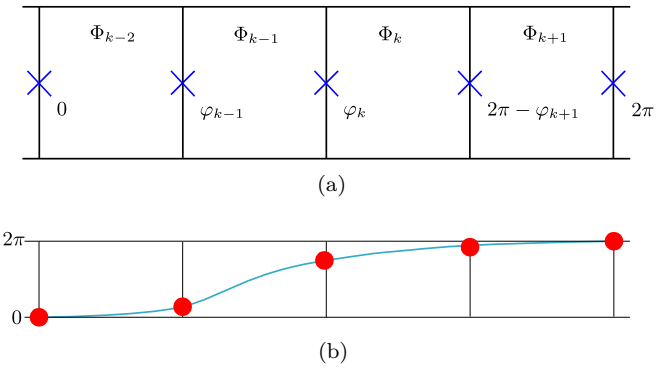

FIG. 2. (a) The highly inductive JJPA with a single trapped MF and (b) the Josephson phase distribution of a small size MF.

Substituting such Josephson phase configuration in (4) we obtain the effective potential energy $U_{\rm eff}$ as follows (here, we consider a specific case $I = 0$):

$$U_{\rm eff}[\{\varphi_i\}_{\rm MF}] = E_J(3-\cos\varphi_{k-1}-\cos\varphi_k-\cos[\varphi_{k+1}])$$
$$+ E_L\left[\left(-\varphi_{k-1}+2\pi\frac{\Phi_{k-2}}{\Phi_0}\right)^2\right.$$
$$+\left(-\varphi_{k+1}+2\pi\frac{\Phi_{k+1}}{\Phi_0}\right)^2$$
$$+\left(\varphi_{k-1}-\varphi_k+2\pi\frac{\Phi_{k-1}}{\Phi_0}\right)^2$$
$$\left.+\left(\varphi_k-2\pi+\varphi_{k+1}+2\pi\frac{\Phi_k}{\Phi_0}\right)^2\right]. \quad (5)$$

Since we are interested in the low-frequency dynamics of Josephson phases, and the Josephson phases $\varphi_{k\pm1}$ display the high-frequency dynamics only, one can expand the potential $U_{\rm eff}$ up to second order in $\varphi_{k\pm1}$ and minimize the potential energy with respect to them. Using this procedure we write the effective potential $U_{\rm eff}(\varphi_k)$ depending on a single macroscopic degree of freedom φ_k, in the following form:

$$U_{\rm eff}(\varphi_k) = E_J(1-\cos\varphi_k)$$
$$+ 2E_L\left(\varphi_k - \pi\left[1+\frac{\Phi_{k-1}-\Phi_k}{\Phi_0}\right]\right)^2 \quad (6)$$

Here for simplicity we set the externally applied magnetic fluxes Φ_{k-2} and Φ_{k+1} to zero, and the condition, $E_J \gg E_L$ is used. The magnetic fluxes Φ_{k-1} and Φ_k allow one to control the positions and the relative depths of potential minimums, and for a most relevant case as $\Phi_{k-1} - \Phi_k = 0$, the dependence of $U_{\rm eff}(\varphi_k)$ is presented in Fig. 3. In this analysis we neglect the interaction of MF with plasma oscillations in tails of MF, i.e., excitations of φ_{k-1} and φ_{k+1}. This assumption is

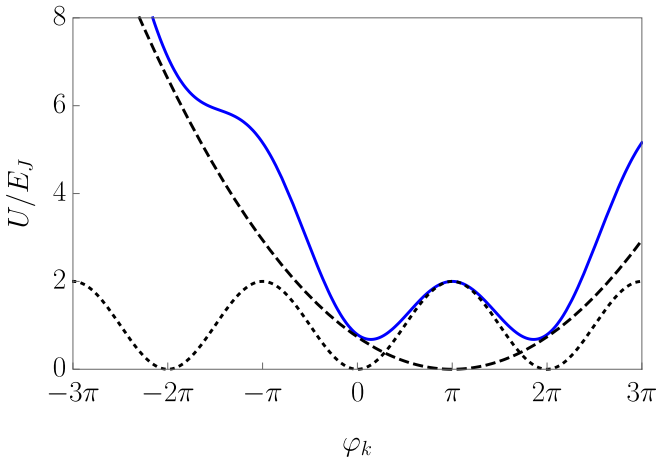

FIG. 3. The effective potential energy $U_{\text{eff}}(\varphi_k)$ (solid blue line) for $\Phi_{k-1} - \Phi_k = 0$. Here, the parameter $E_L = 0.04E_J$ was chosen. Dashed and dotted lines represent parabolic and cos terms in the Eq. (6), respectively.

valid because the strength of such interaction decreases with E_L, and it becomes rather small for typical JJPAs with high kinetic inductances.

Next, we construct the effective periodic potential energy describing the motion of a single MF along a JJPA. First, we use a precise mapping between φ_k and the coordinate x (the center of MF shown by black dots in Fig. 4) defined as $x = d(2\pi - \varphi_k)/(2\pi)$, where d is the size of a single cell, and the origin of x axis is located in the center of $(k-1)$th cell. This procedure illustrated in Fig. 4 allows one to describe the dynamics of MF in the anticontinuous limit by a single collective coordinate x. The potential (6) describing a single MF located in the right half of $(k-1)$th cell [Figs. 4(a), 4(b)] or the left half of kth cell [Fig. 4(c)] of the JJPA, is written down as the $U_{\text{eff}}(x)$ on the interval $0 \leqslant x \leqslant d$.

$$U_{\text{eff}}(x) = E_J\left(1 - \cos\frac{2\pi x}{d}\right) + 2E_L\left(\frac{2\pi x}{d} - \pi\right)^2. \quad (7)$$

Here, we set the magnetic fluxes as $\Phi_{k-1} - \Phi_k = 0$.

Expanding the $U_{\text{eff}}(x)$ in Fourier series we obtain the potential energy of a single MF, which is valid on a whole axis x [Fig. 4(d) indicates the MF with the coordinate $x > d$]:

$$U_{\text{MF}}(x) = \frac{2E_L\pi^2}{3} + E_L\sum_{n=1}^{\infty}\frac{8}{n^2}\cos\frac{2\pi nx}{d} + E_J\left(1 - \cos\frac{2\pi x}{d}\right). \quad (8)$$

The sum can be also expressed as

$$U_{\text{MF}}(x) = 2E_L\left(\frac{\pi^2}{3} + 2\,\text{Li}_2[e^{i\frac{2\pi x}{d}}] + 2\,\text{Li}_2[e^{-i\frac{2\pi x}{d}}]\right) + E_J\left(1 - \cos\frac{2\pi x}{d}\right), \quad (9)$$

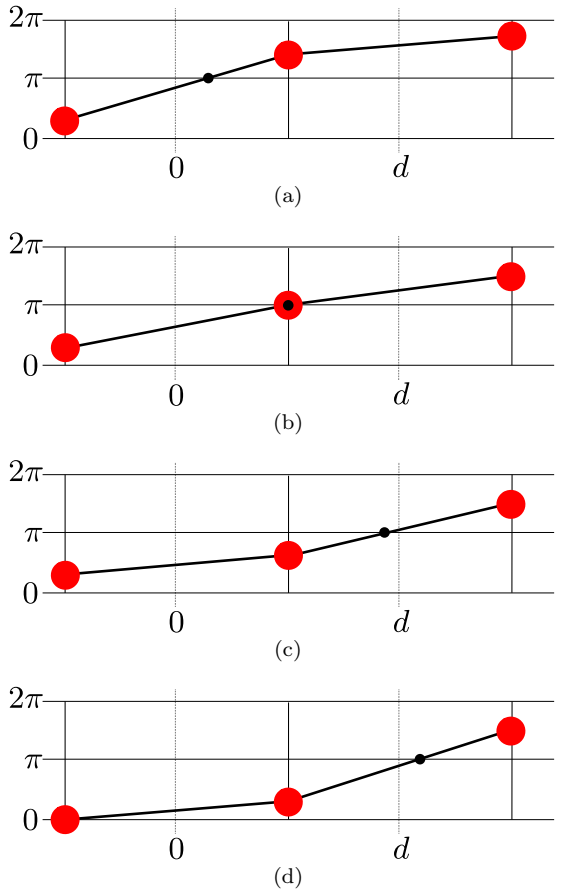

FIG. 4. The snapshots of the Josephson phase distribution of a small size MF. The MF motion from (a) left cell to (c), (d) right cell is shown. The mapping between the Josephson phases (indicated by red circles) and continuous variable (indicated by black dots) is presented.

where

$$\text{Li}_s(z) = \sum_{k=1}^{\infty}\frac{z^k}{k^s} \quad (10)$$

is the polylogarithm function [37]. The potential $U_{\text{MF}}(x)$ is presented in Fig. 5.

The same procedure was used for a single MF in the presence of charging energy, i.e., the kinetic energy term in (1), and externally applied current I in order to obtain the Lagrangian of a single MF trapped in a JJPA

$$L = \frac{E_J(2\pi)^2}{2\omega_p^2 d^2}(\dot{x} - \alpha V_g)^2 - \frac{2E_L\pi^2}{3} - E_L\sum_{n=1}^{\infty}\frac{8}{n^2}\cos\frac{2\pi nx}{d} - E_J\left(1 - \cos\frac{2\pi x}{d}\right) - E_J\frac{I}{I_c}\frac{2\pi x}{d}, \quad (11)$$

where $\alpha = edC_g/(\pi\hbar C)$.

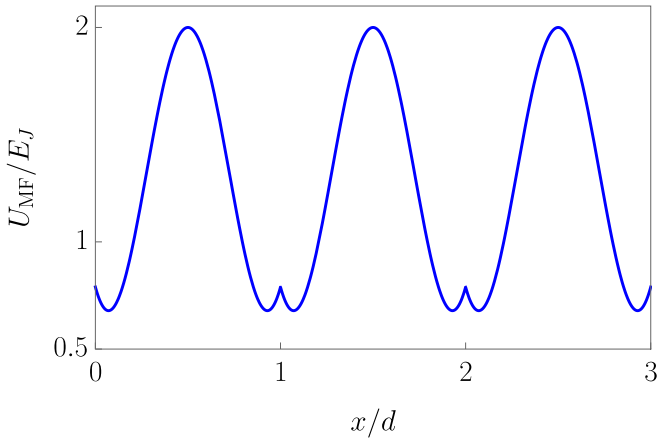

FIG. 5. Spatial dependence of the potential $U_{\rm MF}(x)$ [Eq. (8)]. The parameter $E_L = 0.04E_J$ was chosen.

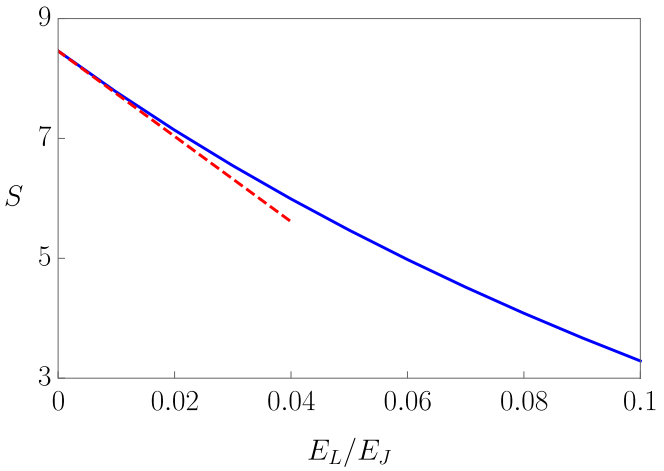

FIG. 6. The dependence of the lowest band width $S = \ln[2\Delta/(\hbar\omega)]$ on the JJPAs dimensionless inductive energy, E_L/E_J. Solid line: exact numerical result; dashed line: linear approximation (14). The parameters are chosen as $E_C = 0.1E_J$, $E_J/(\hbar\omega_p) = 1$.

IV. MACROSCOPIC QUANTUM EFFECTS IN THE COHERENT DYNAMICS OF A SINGLE MF

Introducing the operator of momentum as $\hat{P} = -i\hbar d/dx$ we write the Hamiltonian of a single trapped MF as

$$\hat{H} = \frac{(\hat{P} + m\alpha V_g)^2}{2m} + \frac{2E_L\pi^2}{3} + E_L\sum_{n=1}^{\infty}\frac{8}{n^2}\cos\frac{2\pi n\hat{x}}{d} + E_J\left(1 - \cos\frac{2\pi\hat{x}}{d}\right) + E_J\frac{I}{I_c}\frac{2\pi\hat{x}}{d}, \tag{12}$$

where we define the effective mass of MF, $m = E_J(2\pi)^2/(\omega_p d)^2$.

A. Energy bands

In the absence of both externally applied current I and the gate voltage V_g the coherent quantum dynamics of a single MF is reduced to the quantum dynamics of a single quantum particle moving in the periodic potential $U_{\rm MF}(x)$ (9). It is well known that the eigenfunctions of such quantum problem are determined by the quasimomentum p, and the energy spectrum $E_s(p)$ is composed of infinite number of bands [38]. Moreover, the lowest energy band has a simple form as $E_0(p) = E_0 - \Delta\cos(pd/\hbar)$, where $E_0 \simeq E_J$, and the corresponding eigenfunctions are $\psi_p(n) = (1/\sqrt{M})\exp(ipdn/\hbar)$, where $n = 0, \pm1, \pm2\ldots$ is the cell number of JJPAs. In the limit of $E_J \gg E_C$ the width of energy band Δ is exponentially small, and the parameter Δ determined by tunneling between adjacent potential wells of $U_{\rm MF}(x)$, is obtained in the quasiclassical approximation as [31,39,40]

$$\Delta = \frac{\hbar\omega_0}{2}\exp[-S]$$
$$S = \frac{1}{\hbar}\int_{x_1}^{x_2}\sqrt{2m|U_{\rm MF}(x) - U_{\rm MF}(x_1)|}dx, \tag{13}$$

where x_1 and x_2 are minimums of the potential $U_{\rm MF}(x)$ on the interval $0 < x < d$, and ω_0 is the frequency of small oscillations, $\omega_0 \simeq \omega_p$. Numerically calculating the integral in (13) we obtain the dependence of parameter $S = \ln[2\Delta/(\hbar\omega_0)]$ on $\beta_L = E_J/E_L \geqslant 1$, and this dependence is shown in Fig. 6 (solid line). As the parameter β_L is extremely large, i.e., $\beta_L \gg 1$, we obtain in a linear approximation (see details of calculation in the Appendix A):

$$S = S_0\left(1 - \frac{7\zeta(3)}{\beta_L}\right), \quad S_0 = \frac{8E_J}{\hbar\omega_p}. \tag{14}$$

This dependence is shown in Fig. 6 by dashed line.

B. Coherent quantum oscillations of MF in long linear JJPAs

At low temperatures as the excitations to upper energy bands are strongly suppressed, for long linear JJPAs [see, Fig. 1(a)] the quantum dynamics of MF demonstrates the wave function spreading, and the time-dependent probability $P_l(x,t)$ to obtain MF at the position with coordinate x is written as

$$P_l(x,t) = \left|d\int_{-\infty}^{\infty}\frac{dp}{2\pi\hbar}\exp\left[-\frac{i\Delta}{\hbar}t\cos\frac{pd}{\hbar} - \frac{ipx}{\hbar}\right]\right|^2, \tag{15}$$

and, e.g., the probability to find the MF in the center of n-cell varies with time as $P_l(n,t) = J_n^2(\Delta t/\hbar)$ displaying the decaying quantum beats with the frequency of the order $\hbar/\Delta$. The time-dependent probability to obtain the MF at the initial position, i.e., the center of zeroth cell, is shown in Fig. 7.

C. Coherent quantum dynamics of MF in a short annular JJPA: The Aharonov-Casher phase

Here, we consider the coherent quantum dynamics of MF trapped in a short annular JJPA in the presence of an externally applied gate voltage V_g but the current bias I is still absent. As one can see from the Hamiltonian (12) the amplitude of coherent tunneling of MF between the neighboring cells accumulate the additional phase $\pm\chi$, where $\chi = md\alpha V_g/\hbar$, and the positive (negative) sign corresponds to the tunneling in clockwise (anticlockwise) direction [41]. The phase χ is the seminal Aharonov-Casher phase intensively studied previously in quantum dynamics of magnetic vortices trapped in superconductors or two-dimensional arrays of

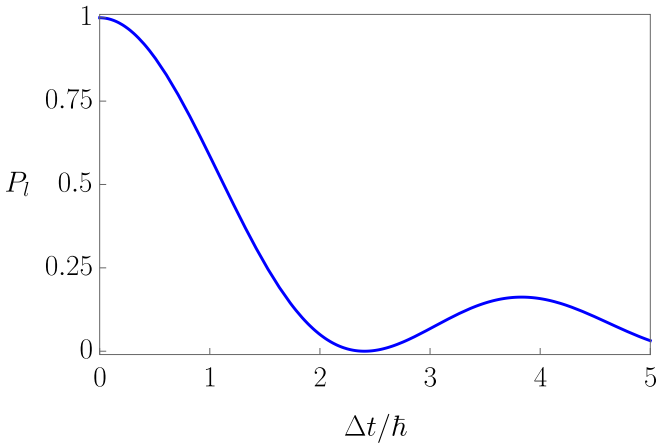

FIG. 7. The time-dependent probability of $P_l(0,t)$ to obtain quantum MF at the initial position in a long linear JJPA.

Josephson junctions [10,29,42,43] or various n-Josephson junctions SQUIDs [41,44].

For a single MF trapped in an annular JJPA with M cells [see Fig. 1(b)] the eigenfunctions of MF are $\psi_{p_m}(n) = (1/\sqrt{M})\exp(ip_m dn/\hbar)$, where $p_m = 2\pi m/M$, $m = 0, 1, 2, \ldots, M-1$, and the energy spectrum of the lowest band $E_0(p_m)$ controlled by the Aharonov-Casher phase χ, has the following form:

$$E_0(p_m) = E_0 - \Delta\cos(p_m d/\hbar + \chi). \tag{16}$$

The coherent quantum dynamics of MF in short annular JJPAs of a size M is completely described by probabilities $P_M(n,t)$ to obtain MF in the n cell at time t if MF was initially located in the zeroth cell. Such probabilities are obtained as follows:

$$P_M(n,t) = \frac{1}{M^2}\left|\sum_{m=0}^{M-1}\exp\left[i\frac{2\pi mn}{M} - i\frac{\Delta t}{\hbar}\cos\left(\frac{2\pi m}{M} + \chi\right)\right]\right|^2 \tag{17}$$

Thus, for $M = 2$ we obtain $P_{M=2}(0,t) = \cos^2[\Delta\cos(\chi)t/\hbar]$, and therefore, for $\chi = 0$ the quantum beats with the frequency of $f_{qb} = \Delta/h$ are realized, but for $\chi = \pi/2$ the quantum beats are completely suppressed, and MF is localized in the zeroth cell. The typical dependencies of $P_M(0,t)$ for annular JJPAs of different sizes ($M = 4, 5$) and a few values of χ are presented in Fig. 8. Notice here, that for $M = 4$ the dependencies $P_{M=4}(0,t)$ for $\chi = 0$ and $\chi = \pi/2$ accidentally coincide.

The location of MF and corresponding quantum oscillations for both long and short JJPAs of different geometries can be experimentally verified by the spectroscopy of plasma excitations interacting with a single MF as it was proposed in Ref. [23].

V. WEAKLY INCOHERENT QUANTUM DYNAMICS OF A SINGLE MF

In the presence of externally applied current $I(t)$, the weakly dissipative dynamics of a single quantum MF trapped in a JJPA of large kinetic inductances can be described as follows: by making use of the quasimomentum p representation we obtain the operator of MF center $\hat{x}$ as $\hat{x} = -i\hbar d/dp$. A

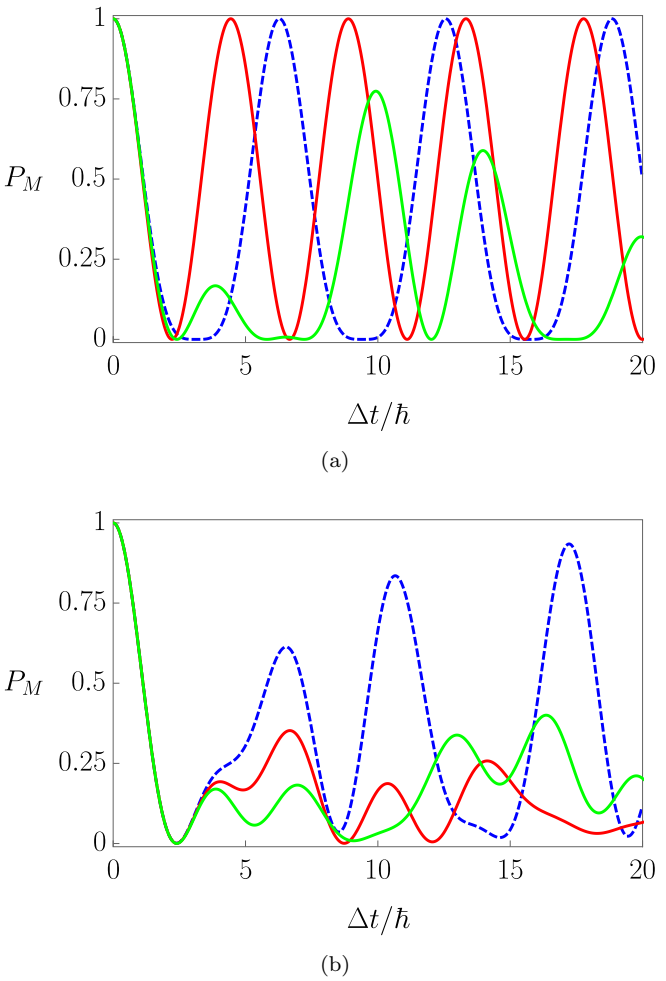

FIG. 8. The time-dependent probability of $P_M(0,t)$ to obtain the quantum MF at the initial position in short annular JJPAs of different sizes: (a) $M = 4$ and (b) $M = 5$. The values of Aharonov-Casher phase χ are chosen as $\chi = 0$ (dashed lines), $\chi = \pi/8$ [green (light gray) solid lines] and $\chi = \pi/4$ [red (gray) solid lines].

weak dissipation can be modeled as the interaction of the MF degree of freedom x with the bath of harmonic oscillators y_i [45]. The total Hamiltonian is $\hat{H}_{tot} = \hat{H} + \hat{H}_{osc} + \hat{H}_{\rm int}$, where the interaction Hamiltonian is determined as $\hat{H}_{\rm int}(x, y_i) = g\hat{x}\sum_i \hat{y}_i$ [45,46]. In this case the Heisenberg equation of motion for the operator $\dot{\hat{x}}$ is written as

$$\dot{\hat{x}} = \left[\frac{d}{d\hat{p}}, \hat{H}\right] = \frac{dE_s(\hat{p})}{d\hat{p}}, \tag{18}$$

where $E_s(p)$ are the energy bands of the macroscopic quantum particle moving in the potential, $U_{\rm MF}(x)$ [see, Eq. (8)]. In the presence of dissipation the Heisenberg equation of motion for the operator $\hat{p}$ is written as

$$\dot{\hat{p}} = -\frac{1}{\hbar}[\hat{p}, \hat{H}] - \frac{1}{\hbar}[\hat{p}, \hat{H}_{\rm int}], \tag{19}$$

For a weakly dissipative case we can trace out the bath degrees of freedom [30,46], and obtain the equation of motion:

$$\dot{\hat{p}} = \frac{2\pi E_J}{dI_c}I(t) - \gamma m\dot{\hat{x}}. \tag{20}$$

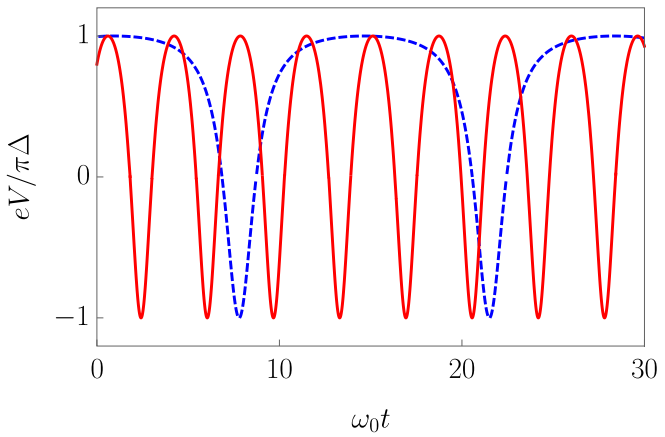

FIG. 9. The periodic dependence of the voltage, $V(t)$, on time for two values of parameter I/I_t, i.e., $I/I_t = 1.1$ (dashed line) and $I/I_t = 2$ [red (gray) solid line].

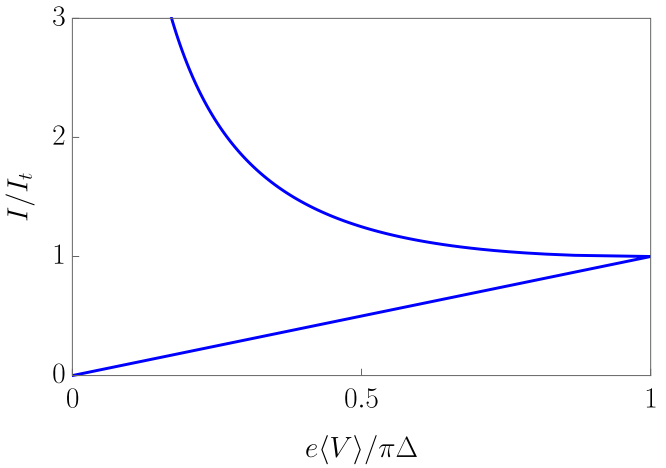

FIG. 10. The nose-type of current-voltage characteristics of JJPAs with a single MF.

Here, we introduce the phenomenological parameter γ (the inverse relaxation time) characterizing the interaction of the moving topological MF with the environment, i.e., dissipation and decoherence processes. Substituting (18) in (20), we obtain the dynamic equation for the quantum MF as

$$\dot{p} = \frac{2\pi E_J}{dI_c} I(t) - \gamma m \frac{dE_s(p)}{dp}. \tag{21}$$

Since voltage V is determined by the Josephson relationship as $2eV = \hbar\dot{\varphi} = (2\pi\hbar/d)\dot{x}$, and using (18) we obtain the expression for the voltage as

$$V = \frac{\pi\hbar}{ed}\frac{dE_s(p)}{dp}. \tag{22}$$

Notice here that a similar analysis has been carried out long time ago in Refs. [30,31] for small Josephson junctions subject to applied external current I.

1. Bloch oscillations and current-voltage characteristics

First, we analyze the weakly dissipative dynamics of a single MF in the presence of applied dc current, I. The Eq. (21) has a stationary solution $\dot{p} = 0$ as $I < I_t$, where

$$I_t = \frac{2\pi\gamma\Delta}{\hbar\omega_p^2} I_c. \tag{23}$$

In this regime the voltage V linearly depends on the current I as $V = [\hbar\omega_p^2/(2eI_c\gamma)]I$. As the current $I > I_t$ the solution $p(t)$ of (21) is a nonstationary one, and by taking into account a single lowest energy band we obtain the solution analytically (see details in Appendix B). In this regime the voltage depends periodically on time (see Fig. 9), and the period T (see Appendix B) is written as

$$T = \frac{2\pi}{\omega_0}\frac{I_t}{\sqrt{I^2 - I_t^2}}, \quad I > I_t \tag{24}$$

where we introduce the typical frequency of MF Bloch oscillations, $\omega_0 = (2\pi)^2 E_J\gamma\Delta/(\omega_p\hbar)^2 = \pi I_t/e$. Notice here that the period T increases up to infinity as the current I approaches I_t. Substituting the solution of the dynamic equation [see Eq. (B2)] to (22) we obtain the voltage $V(t)$ oscillating in time with the frequency, $f_{Bl} = \sqrt{I^2 - I_t^2}/(2e)$. The dependence of $V(t)$ displaying the periodic Bloch oscillations with the frequency f_{Bl}, is presented in Fig. 9 for two different values of I/I_t.

Averaging the voltage $V(t)$ over the period allows one to obtain the universal form of the current-voltage characteristics (the I-V curve):

$$\langle V\rangle = \frac{\pi\Delta}{e}\cdot\frac{I - \sqrt{I^2 - I_t^2}}{I_t}, \quad I > I_t$$
$$\langle V\rangle = \frac{\pi\Delta}{e}\cdot\frac{I}{I_t}, \quad I < I_t. \tag{25}$$

Such nose type of I-V curve [30,31] is the fingerprint of Bloch oscillations in the dynamics of a quantum MF in a JJPA of large kinetic inductances, and it is presented in Fig. 10. In this analysis we neglect the Landau-Zener transitions to upper bands, and since the probability of such transitions is determined as $p_{LZ} \simeq \exp[-\pi(\omega_p)^2 md/F]$, where F is the slope of the effective potential [the last term in the Eq. (11)], this approximation is valid as $I \ll I_c$. In the presence of both dc current I and ac current with the frequency f, the seminal current steps located at $I_n = 2enf$ can be obtained [30,31].

VI. CONCLUSION

In conclusion, we studied in detail various phenomena occurring in macroscopic quantum dynamics of a topological MF trapped in JJPAs with high kinetic inductances. An implementation of high kinetic inductances in the form of series arrays of large Josephson junctions allows one to elegantly solve two problems, i.e., reducing drastically the MF size less than the size of a single cell d and diminishing the low-frequency offset charge noise [20,22]. In this case the quantum dynamics of a single MF is precisely described by a single degree of freedom, i.e., the coordinate of the MF center x. By using such description we obtain the MF effective mass m, the MF effective kinetic energy controlled by the gate voltage V_g, the MF effective potential energy that, in turn, depends on the externally applied current I [see Eq. (11)]. In the absence of externally applied current I the effective

potential depends periodically on the coordinate x, and the energy spectrum of MF contains of infinite number of energy bands. The width of the lowest energy band, Δ, increases with the inductive energy E_L (see Fig. 6). For long linear JJPAs [see the schematic in Fig. 1(a)] the parameter Δ determines the typical frequency of decaying quantum oscillations in the MF wave packet spread (see Fig. 7). For short annular JJPAs [see the schematic in Fig. 1(b)] the coherent quantum dynamics of MF demonstrates complex quantum oscillations controlled by an external gate voltage V_g through the Aharonov-Casher phase $\chi \propto V_g$ (see Fig. 8). In particular, we obtain that for a two-cells annular JJPA the frequency of quantum beats is determined as $f_{\rm qb} = \Delta\cos(\chi)/h$, and therefore, for $\chi = \pi/2$ the quantum beats are completely suppressed. These quantum oscillations can be experimentally observed through the spectroscopy of plasma oscillations as it was proposed in Ref. [23].

As the external dc bias current $I < I_c$ is applied the quantum dynamics of MF displays the seminal Bloch oscillations in the time dependence of the voltage $V(t)$ (see, Fig. 9). These Bloch oscillations result in the nose-type I-V curves (Fig. 10), and the current steps as both dc and ac currents are applied. Finally, we notice that the Bloch oscillations and the current steps in the current-voltage characteristics are very sensitive to the offset charge noise, and, therefore, the JJPAs with large kinetic inductances in which the charge fluctuations are shunted [20,22] can be used for the field of quantum metrology with topological MFs.

ACKNOWLEDGMENTS

We thank S. Mukhin and A. Ustinov for valuable discussions. This work was financially supported by the Russian Science Foundation, Project No. 19-42-04137.

APPENDIX A: ANALYTICAL CALCULATION OF THE ENERGY BAND WIDTH AS $\beta_L \gg 1$

To obtain the energy band width in the limit of $\beta_L \gg 1$ we expand S up to the first order in E_L:

$$S \approx \frac{1}{\hbar}\int_0^d \sqrt{2mE_J\left(1-\cos\frac{2\pi x}{d}\right)}dx - \sqrt{\frac{2m}{E_J}}\frac{4E_L\pi^2}{\hbar d^2}\int_{x_1}^{x_2}\frac{(x-d+dx_1)(x-dx_1)}{\sqrt{\cos\frac{2\pi x_1}{d}-\cos\frac{2\pi x}{d}}}dx. \quad \text{(A1)}$$

The first integral in (A1) was calculated exactly:

$$S_0 = \int_0^d \sqrt{2mE_J\left(1-\cos\frac{2\pi x}{d}\right)}dx = \frac{4\sqrt{mE_J}d}{\pi} = \frac{8E_J}{\hbar\omega_p}. \quad \text{(A2)}$$

The dependence of S on E_L is written as

$$S = S_0 - \sqrt{\frac{2m}{E_J}}\frac{4\pi^2}{\hbar d^2}I(E_L), \quad \text{(A3)}$$

where

$$I(E_L) = \int_{\eta E_L}^{d-\eta E_L}\frac{(x-d+d\eta E_L)(x-d\eta E_L)}{\sqrt{\cos\frac{2\pi\eta E_L}{d}-\cos\frac{2\pi x}{d}}}dx. \quad \text{(A4)}$$

Here, the limits of integration are written as

$$x_1 \approx 0+\eta E_L$$
$$x_2 \approx d-\eta E_L. \quad \text{(A5)}$$

The exact expression of η is not important here. In the first-order approximation over E_L one can obtain

$$S = S_0 - \sqrt{\frac{2m}{E_J}}\frac{4\pi^2}{\hbar d^2}I(0), \quad \text{(A6)}$$

and the integral $I(0)$ is calculated explicitly as

$$I(0) = \frac{7d^3\zeta(3)}{\sqrt{2}\pi^3} \approx 0.19d^3, \quad \text{(A7)}$$

where $\zeta(x)$ is the Riemann zeta function [37].

APPENDIX B: CURRENT-VOLTAGE CHARACTERISTICS OF JJPA WITH A TRAPPED QUANTUM MF

Introducing the dimensionless variables, i.e., $z = pd/\hbar$ and $\tau = \omega_0 t$, we obtain the dynamic equation in the following form:

$$\frac{dz}{d\tau} = \frac{I}{I_t} - \sin(z). \quad \text{(B1)}$$

For $I > I_t$ the solution of Eq. (B1) is written as

$$z(\tau) = 2\arctan\left[\frac{\sqrt{a^2-1}\tan\frac{(\tau-\tau_0)\sqrt{a^2-1}}{2}+1}{a}\right], \quad \text{(B2)}$$

where $a = I/I_t > 1$ and τ_0 is determined by the initial condition. This solution increases with time and periodically oscillates with the dimensionless period $\tilde{T} = 2\pi/\sqrt{a^2-1}$.

[1] T. Dauxois and M. Peyrard, *Physics of solitons* (Cambridge University Press, Cambridge, 2006).
[2] Y. V. Kartashov, B. A. Malomed, and L. Torner, Solitons in nonlinear lattices, Rev. Mod. Phys. **83**, 247 (2011).
[3] A. C. Scott, Solitons in biological molecules, *Emerging Syntheses in Science* (CRC Press, 2018).
[4] N. Manton and P. Sutcliffe, *Topological Solitons* (Cambridge University Press, Cambridge, 2004).

[5] Y. S. Kivshar and B. A. Malomed, Dynamics of solitons in nearly integrable systems, Rev. Mod. Phys. **61**, 763 (1989).

[6] A. Ustinov, Solitons in josephson junctions, Physica D **123**, 315 (1998).

[7] I. Vernik, N. Lazarides, M. So/rensen, A. Ustinov, N. F. Pedersen, and V. Oboznov, Soliton bunching in annular josephson junctions, J. Appl. Phys. **79**, 7854 (1996).

[8] A. Wallraff, A. V. Ustinov, V. V. Kurin, I. A. Shereshevsky, and N. K. Vdovicheva, Whispering Vortices, Phys. Rev. Lett. **84**, 151 (2000).

[9] M. V. Fistul and A. V. Ustinov, Libration states of a nonlinear oscillator: Resonant escape of a pinned magnetic fluxon, Phys. Rev. B **63**, 024508 (2000).

[10] R. Fazio and H. Van Der Zant, Quantum phase transitions and vortex dynamics in superconducting networks, Phys. Rep. **355**, 235 (2001).

[11] H. S. J. Van der Zant, W. J. Elion, L. J. Geerligs, and J. E. Mooij, Quantum phase transitions in two dimensions: Experiments in josephson-junction arrays, Phys. Rev. B **54**, 10081 (1996).

[12] T. Kato and M. Imada, Macroscopic quantum tunneling of a fluxon in a long josephson junction, J. Phys. Soc. Jpn. **65**, 2963 (1996).

[13] Z. Hermon, A. Stern, and E. Ben-Jacob, Quantum dynamics of a fluxon in a long circular josephson junction, Phys. Rev. B **49**, 9757 (1994).

[14] A. Shnirman, E. Ben-Jacob, and B. Malomed, Tunneling and resonant tunneling of fluxons in a long josephson junction, Phys. Rev. B **56**, 14677 (1997).

[15] A. Wallraff, Y. Koval, M. Levitchev, M. Fistul, and A. Ustinov, Annular long josephson junctions in a magnetic field: engineering and probing the fluxon interaction potential, J. Low Temp. Phys. **118**, 543 (2000).

[16] A. Wallraff, A. Lukashenko, J. Lisenfeld, A. Kemp, M. Fistul, Y. Koval, and A. Ustinov, Quantum dynamics of a single vortex, Nature (London) **425**, 155 (2003).

[17] Y. Nakamura, Y. A. Pashkin, and J. S. Tsai, Coherent control of macroscopic quantum states in a single-Cooper-pair box, Nature (London) **398**, 786 (1999).

[18] M. B. Metcalfe, E. Boaknin, V. Manucharyan, R. Vijay, I. Siddiqi, C. Rigetti, L. Frunzio, R. J. Schoelkopf, and M. H. Devoret, Measuring the decoherence of a quantronium qubit with the cavity bifurcation amplifier, Phys. Rev. B **76**, 174516 (2007).

[19] P. Krantz, M. Kjaergaard, F. Yan, T. P. Orlando, S. Gustavsson, and W. D. Oliver, A quantum engineer's guide to superconducting qubits, Appl. Phys. Rev. **6**, 021318 (2019).

[20] V. E. Manucharyan, J. Koch, L. I. Glazman, and M. H. Devoret, Fluxonium: Single cooper-pair circuit free of charge offsets, Science **326**, 113 (2009).

[21] K. A. Matveev, A. I. Larkin, and L. I. Glazman, Persistent Current in Superconducting Nanorings, Phys. Rev. Lett. **89**, 096802 (2002).

[22] I. N. Moskalenko, I. S. Besedin, I. A. Tsitsilin, G. S. Mazhorin, N. N. Abramov, A. Grigor'ev, I. A. Rodionov, A. A. Dobronosova, D. O. Moskalev, A. A. Pishchimova *et al.*, Planar architecture for studying a fluxonium qubit, JETP Lett. **110**, 574 (2019).

[23] I. N. Moskalenko, I. S. Besedin, S. S. Seidov, M. V. Fistul, and A. V. Ustinov (unpublished).

[24] N. Maleeva, L. Grünhaupt, T. Klein, F. Levy-Bertrand, O. Dupre, M. Calvo, F. Valenti, P. Winkel, F. Friedrich, W. Wernsdorfer *et al.*, Circuit quantum electrodynamics of granular aluminum resonators, Nature Commun. **9**, 3889 (2018).

[25] T. M. Hazard, A. Gyenis, A. Di Paolo, A. T. Asfaw, S. A. Lyon, A. Blais, and A. A. Houck, Nanowire Superinductance Fluxonium Qubit, Phys. Rev. Lett. **122**, 010504 (2019).

[26] O. Astafiev, L. Ioffe, S. Kafanov, Y. A. Pashkin, K. Y. Arutyunov, D. Shahar, O. Cohen, and J. S. Tsai, Coherent quantum phase slip, Nature (London) **484**, 355 (2012).

[27] A. Petrescu, H. E. Türeci, A. V. Ustinov, and I. M. Pop, Fluxon-based quantum simulation in circuit qed, Phys. Rev. B **98**, 174505 (2018).

[28] S. Flach and C. R. Willis, Discrete breathers, Phys. Rep. **295**, 181 (1998).

[29] B. Reznik and Y. Aharonov, Question of the nonlocality of the aharonov-casher effect, Phys. Rev. D **40**, 4178 (1989).

[30] K. Likharev and A. Zorin, Theory of the bloch-wave oscillations in small josephson junctions, J. Low Temp. Phys. **59**, 347 (1985).

[31] G. Schön and A. D. Zaikin, Quantum coherent effects, phase transitions, and the dissipative dynamics of ultra small tunnel junctions, Phys. Rep. **198**, 237 (1990).

[32] U. Vool and M. Devoret, Introduction to quantum electromagnetic circuits, Int. J. Circuit Theory Appl. **45**, 897 (2016).

[33] P. Müller, I. Grigorieva, V. Schmidt, and A. Ustinov, *The Physics of Superconductors: Introduction to Fundamentals and Applications* (Springer, Berlin, 2013).

[34] O. M. Braun and Y. S. Kivshar, Nonlinear dynamics of the frenkel-kontorova model, Phys. Rev. B **43**, 1060 (1991).

[35] B. Joos, Properties of solitons in the frenkel-kontorova model, Solid State Commun. **42**, 709 (1982).

[36] K. Furuya and A. O. de Almeida, Soliton energies in the standard map beyond the chaotic threshold, J. Phys. A: Math. Gen. **20**, 6211 (1987).

[37] M. Abramowitz and I. A. Stegun, *Handbook of Mathematical Functions with Formulas, Graphs, and Mathematical Tables* (Dover, New York, 1964).

[38] L. D. Landau, E. M. Lifšic, E. M. Lifshitz, and L. Pitaevskii, *Statistical Physics: Theory of the Condensed State*, Vol. 9 (Butterworth-Heinemann, Oxford, 1980).

[39] L. D. Landau and L. M. Lifshitz, *Quantum Mechanics Non-Relativistic Theory, Third Edition: Volume 3*, 3rd ed. (Butterworth-Heinemann, 1981).

[40] G. Catelani, R. J. Schoelkopf, M. H. Devoret, and L. I. Glazman, Relaxation and frequency shifts induced by quasiparticles in superconducting qubits, Phys. Rev. B **84**, 064517 (2011).

[41] J. R. Friedman and D. V. Averin, Aharonov-Casher-Effect Suppression of Macroscopic Tunneling of Magnetic Flux, Phys. Rev. Lett. **88**, 050403 (2002).

[42] W. J. Elion, J. J. Wachters, L. L. Sohn, and J. E. Mooij, Observation of the Aharonov-Casher Effect for Vortices in Josephson-Junction Arrays, Phys. Rev. Lett. **71**, 2311 (1993).

[43] B. J. van Wees, Aharonov-Bohm–Type Effect for Vortices in Josephson-Junction Arrays, Phys. Rev. Lett. **65**, 255 (1990).

[44] I.-M. Pop, B. Douçot, L. Ioffe, I. Protopopov, F. Lecocq, I. Matei, O. Buisson, and W. Guichard, Experimental demonstration of aharonov-casher interference in a josephson junction circuit, Phys. Rev. B **85**, 094503 (2012).

[45] A. Caldeira and A. J. Leggett, Quantum tunnelling in a dissipative system, Ann. Phys. (NY) **149**, 374 (1983).

[46] T. Dittrich, P. Hänggi, G.-L. Ingold, B. Kramer, G. Schön, and W. Zwerger, *Quantum Transport and Dissipation*, Vol. 3 (Wiley-Vch, Weinheim, 1998).